

Carbon/Carbon Composite Bipolar Plate for PEM Fuel Cells

Theodore M. Besmann,* James W. Klett, John J. Henry, Jr., and Edgar Lara-Curzio

Metals and Ceramics Division, Oak Ridge National Laboratory, Oak Ridge, Tennessee 37830-6063, USA

Copyright © 2001 Society of Automotive Engineers, Inc.

ABSTRACT

Carbon/carbon-composite bipolar plates for proton-exchange-membrane fuel cells have been fabricated by slurry molding a chopped-fiber preform followed by sealing with chemically vapor-infiltrated carbon. The resulting component is hermetic with respect to through-thickness leakage, has a high electronic conductivity as a result of the deposited graphitic carbon, a low density due to retained porosity, and is corrosion resistant. Biaxial flexure strength was measured to be 175 ± 26 MPa. Cell testing of a 100-cm^2 active area plate indicated low cell resistance and high efficiency.

INTRODUCTION

The significant and growing interest in fuel cells for stationary power and transportation applications has been demonstrated by the attention these technologies are receiving from both government and industry, and particularly from the automotive sector [1]. Interest for vehicular applications has focused on the proton exchange membrane fuel cell (PEMFC) because of its low-temperature operation and thus rapid start-up. Currently, challenges for PEMFC technology for automobiles include reducing the cost and weight of the fuel cell stack, the goal being a 50 kW system of $< \$40/\text{kW}$ and < 133 kg in mass. One of the key components is the bipolar plate, which is the electrode plate that separates individual cells in a stack [2]. The reference design requires the bipolar plate to be high-density graphite with machined flow channels. Both material and machining costs are prohibitive ($\sim \$10/\text{plate}$), and this has led to substantial development efforts to replace graphite. The bipolar plate requirements include low-cost materials and processing (goal of $< \$10/\text{kW}$), light weight, thin ($< 3\text{mm}$), sufficient mechanical integrity, high surface and bulk electronic conductivity, low permeability (boundary between fuel and oxidant), and corrosion resistance in the moist atmosphere of the cell ($< 16 \mu\text{A}/\text{cm}^2$) [3].

The bipolar plate approach developed at Oak Ridge National Laboratory (ORNL) uses a low-cost, slurry-molding process to produce a carbon-fiber preform. The molded, carbon-fiber component could have an inherent volume for diffusing fuel or air to the electrolyte surface

or impressed, flow-field channels. The bipolar plate is made hermetic through chemical vapor infiltration (CVI) with carbon. The infiltrated carbon also serves to make the component highly conductive.

MAIN SECTION

Slurry-Molding. Fibrous component preforms for a sub-scale plate ($120 \times 140 \times 2.5$ mm) are prepared by a slurry molding technique using $10 \mu\text{m}$ -diameter, $100\text{-}\mu\text{m}$ -long carbon fibers (Fortafil 3(c) 00 PAN-based) suspended in water containing phenolic DUREZ[®] resin (Occidental Chemical Corp.) [4]. The fiber-to-phenolic mass ratio is 4:3. A vacuum-molding process produces an ~ 18 vol % fiber, isotropic preform material containing particles of phenolic (Fig. 1). After drying, a set of brass molds fabricated with 0.78 mm (31 mil) deep and wide channels are used to impress these and other features into the preform material at 150°C and a pressure of 10 kPa. The phenolic binder serves to provide green strength and geometric stability after curing in the mold.

Chemical Vapor Infiltration. The surface of the preform is sealed using a CVI technique in which carbon is deposited on the near-surface material in sufficient quantity to make it hermetic. The depth of infiltration is governed by the inherent competition between the kinetics of the surface reactions that produce the deposited material and the mass transport mechanism that allows the reactants to diffuse to the internal volume of the material [5]. The result is that the more rapid the kinetics of deposition as compared to mass transport, the more likely material will be deposited near the surface and the reactants will not significantly penetrate into the thickness of the porous preform. In a review of carbon deposition, Delhaes [6] describes depth penetration of CVI carbon as a function of temperature. The higher the temperature the more rapid the surface deposition kinetics (Arrhenius relationship), thus, the smaller penetration depth allows the surface to be sealed and the bulk volume of the preform to retain a large volume fraction of porosity.

A high surface-to-volume CVI reactor was used to minimize soot formation and allow the efficient infiltration of the fibrous preform (Fig. 2). This design, to some extent, simulates commercial reactors that can accommodate many thousands of parts that fill much of

the free volume. Based on Delhaes [6] and Bammidipati, Stewart, Elliott, Jr., Gokoglu, and Purdy [7], an infiltration temperature of 1500°C was selected with methane (chemically pure, Air Liquide, Houston, TX) as the precursor. Reduced pressure (8 kPa) also suppresses the formation of soot. Flow rates of 1000 cm³/min methane in 2500 cm³/min argon. A processing time on the order of 4 h was determined to be necessary to obtain sealed surfaces. In addition, during the high temperature CVI processing the phenolic present in the preform is pyrolyzed.

Characterization. Bulk electronic conductivity was measured by a four-point probe technique. The four-point probe has a linear configuration with spacing of 1.25 mm between the probes. A known current is applied through the two outermost probes and the resulting voltage across the two innermost probes is measured. Surface resistivity was measured using a test jig that held two sharp probes 2.54 cm apart with four-wire measurements at the probes. The material under test was placed on top of the test jig with a weight on it for consistent connection.

Through-thickness hermeticity was determined using an apparatus that consists of two metal plates between which is fixed the bipolar plate. It is sealed along its periphery with silicone rubber gaskets. An inlet line for hydrogen in one metal plate allows that side to be pressurized to 206 kPa gauge with hydrogen, and an outlet line on the opposite plate allows measurement of any hydrogen flow through the plate using water displacement. The sample was considered sealed if no measurable hydrogen could be collected over a 1 h period. Surfaces were examined using scanning electron microscopy (SEM) (Hitachi S-800) and polished cross-sections were viewed using optical microscopy.

Mechanical properties were measured using a biaxial-flexure apparatus with a ring-on-ring configuration. Samples of material 3.8-cm in diameter (disks) and 1.5-mm in thickness were prepared. The advantage of the biaxial flexure tests over conventional three- and four-point bend tests is that they eliminate undesirable edge failures and are more representative of the loading conditions that would be encountered in application. In this test, the specimen is supported on a coaxial ring and loaded at the center with a smaller ring. For thin (thickness/diameter < 0.1), rigid elastic plates, the radial and tangential stresses are equal and maximum within the loading ring. These stresses are given by:

$$s_{r,q} = \frac{3P}{4t^2} \left(2(1+\nu) \ln \frac{a}{b} + \frac{((1-\nu)(a^2 - b^2))a^2}{a^2 R^2} \right) \quad (1)$$

where P is the applied load, t is the thickness of the specimen, a is the radius of the supporting ring, b is the radius of the loading ring, R is the radius of the specimen, and ν is its Poisson's ratio, for which a value of 0.2 was used [8,9].

The fixture, schematically shown in Fig. 3, was used for the tests that were conducted under a constant cross-head displacement rate of 20 μ m/sec. To insure

continuous contact between the specimen and the fixture (because the specimens were not perfectly flat), silicone "o"-rings were used as loading rings along with a thin layer of vacuum grease between the rings and the specimen to minimize friction. The mid-diameter of the outer ring was 33 mm whereas that of the inner ring was 16.5 mm. Both silicone "o"-rings were 2 mm thick. Acoustic emissions were recorded during the test and correlated to the applied load using a Physical Acoustic Inc. system (model Locan 420D) by contacting a sensor to the bottom of the specimen using vacuum grease.

PEMFC and Corrosion Testing. A 100-cm² active area plate was tested in a PEMFC system with both air and hydrogen at 206 kPa gauge pressure and twice the stoichiometric flows (at 1 A/cm²). A W. L. Gore & Associates (Elkton, MD) Primea membrane and electrode assembly with about 0.1 mg Pt/cm² on the anode side and about 0.3 mg Pt/cm² on the cathode side was used with E-Tek (Natick, MA) backings. The anode humidifier was at 105°C and the cathode humidifier was at 80°C. Dissolution characteristics were determined from polarization curves. These measurements were performed at 80°C in the following solution: 0.001 N H₂SO₄, 2 ppm F⁻ with a nitrogen purge.

RESULTS

A fabricated 100-cm² active area plate is seen in Fig. 4, exhibiting a molded flow field. This is viewed in a polished cross-section in Fig. 5 which also shows the molded channels. Deposited carbon can be seen coating the fibers within the highly porous region. Material density is ~0.96 g/cm³ from mass and geometrical measurements.

Bulk conductivity was measured to be 200-300 S/cm, with lower measurements typically obtained on the more porous side, and a surface resistivity of 12.2±4.2 Ω /cm was determined. These values can be compared to those of a high density graphite, POCO AXF-5Q (POCO, Decatur, Texas) which has a bulk conductivity as reported by POCO of 680 S/cm and an ORNL-measured surface resistivity of 7.8±2.62 Ω /cm.

The bipolar plates are typically slightly warped after infiltration, perhaps due to the slightly (\leq 5%) non-uniform deposition of carbon across the surface. The thin, infiltrated layer and fiber-reinforced nature of the material, however, make it sufficiently pliable that the plate can be flexed without failing. Plates provided for cell testing were, of necessity, pressed flat in the cell without cracking or leaking.

The mechanical properties of the bipolar plate material were tested in biaxial flexure. An example of the stress versus cross-head displacement/acoustic emission results is seen in Fig. 6. The recorded cross-head displacement includes contributions from the deflection of the specimen, the compliance of the support rings, the fixture, and the load train. To determine if the acoustic emissions recorded at relatively low loads were the result of cracks that caused

the material to lose hermeticity, samples were subjected to 100 MPa stresses and acoustic signals observed. The samples were then tested for hermeticity by pressurizing one side with 206 kPa of hydrogen and measuring the through-thickness gas leakage rate. They were determined to not have failed when no measurable (by water displacement) hydrogen could be collected from the low pressure side over 1 h. The average ultimate biaxial flexure strength was 175 ± 26 MPa (25.3 ± 3.8 ksi) as compared to the reported flexural strength by POCO Inc. for AXF-5Q, which has a density of 1.78 g/cm^3 , of 86 MPa (12.5 ksi).

To evaluate the effect of freezing and thawing of water in the bipolar plate structure, a machined flow-field plate was saturated with water and allowed to freeze. The plate was then thawed and dried with no apparent mechanical failure per visual inspection.

A 100-cm^2 active area plate was utilized in a PEMFC and exhibited the characteristics seen in Fig. 7. The cell resistance was not as low as expected, but only a small percentage of the resistance attributable to the bipolar plate material as there was thought to be poor contact between the plate and other components. The current-voltage behavior up to moderately high currents indicated good fuel-air distribution, although there is believed to be leakage from seals around the edge of the plate in the cell requiring higher than typical flows to be used.

To determine corrosion potential, polarization curves were obtained for both sides of the composite carbon sample. A curve for AXF-5Q POCO graphite was generated for comparison. At an open circuit air electrode potential of 1 V vs. NHE, the corrosion current was nearly two orders of magnitude less than for POCO graphite. A long-term test was performed to determine whether surface resistance would change with time. A current of 1 A/cm^2 was passed through the sample while hydrogen and air were bubbled through the electrolyte compartments on opposite sides of the specimen. During the 2000-hour test, resistance at both the anode and cathode changed less than 0.001 ohm-cm^2 .

DISCUSSION

Property and cost targets and comparative figures for POCO graphite and the composite bipolar plate are shown in Table I. The exceptionally high electronic conductivity of the composite material is due to the graphitic carbon deposited at relatively high temperatures. The carbon coats the fibers throughout the component providing a highly conductive electrical path through the thickness and along the surface.

The preferred orientation of the deposited carbon is helpful in preserving the integrity of the material under stress. Vapor-deposited, graphitic carbon has a preferred crystallographic orientation such that the *c* direction of the hexagonal structure is normal to the deposition surface [5]. The basal planes lie parallel to the surface so that cracks are more likely directed along the surface rather than through the thickness. Such

cracks were most likely the source of the acoustic emissions detected at less than ultimate strength during biaxial flexure testing.

The channel walls in the cross-sections of the bipolar plate are not as smooth and even as would be desirable (Fig. 5). This is likely due to the un-optimized mold and molding conditions.

The PEMFC testing of the bipolar plate demonstrated very good performance with high reactant distribution indicating that both the material and its configuration work well. Corrosion rates were also very low, and significantly less than for the standard graphite material.

The ability to emboss or impress features into a preform material is key to eventual large-scale production and that has been demonstrated. It is expected that the material could be produced using a continuous process analogous to paper-making, and that penetrations, channels, and other features could be directly applied as was demonstrated in this work. Preliminary estimates of total costs indicate a 23- x 23-cm plate could be produced in high volume for $<\$2/\text{unit}$. This includes current materials cost (fiber, phenolic resin) of $\$0.12/\text{plate}$, estimate of batch preform processing cost of $\$0.26/\text{plate}$ and CVI cost of $\$1/\text{plate}$ (B.F. Goodrich Corp. quote for batch processing of 30,000 plates). It is envisioned that large-scale production would afford greater cost reductions through the utilization of continuous preform production and perhaps even continuous CVI with preforms traveling through a tunnel furnace for infiltration.

CONCLUSION

The proposed carbon/carbon-composite bipolar plate material has very promising fabrication, material, and performance characteristics. The measured strengths are high and the retention of hermeticity even after damage accumulation is important. One of the most critical characteristics for transportation applications is its low weight, which is approximately half that of other potential materials. The high electronic conductivity may also be important for PEMFC efficiency. Finally, the potential fabrication routes for the component lend themselves to continuous processes and economies of scale, so costs should not be a barrier to use of the material in most PEMFC applications.

ACKNOWLEDGMENTS

The authors would like to thank D. F. Wilson and M. P. Brady for reviewing the manuscript and their suggestions. M. S. Wilson and Z. Zawodzinski of Los Alamos National Laboratory performed the bulk electrical conductivity and fuel cell performance measurements and K. Weisbrod of Los Alamos National Laboratory made the corrosion measurements. This research was supported by the U. S. Department of Energy, Energy Efficiency and Renewable Energy,

REFERENCES

1. T. F. Fuller, *Interface*, Fall 1997, 26 (1997).
2. T. R. Ralph, *Platinum Metals Rev.*, **41** (3), 102 (1997).
3. R. L. Borup and N. E. Vanderborgh in *Materials for Electrochemical Energy Storage and Conversion – Batteries, Capacitors and Fuel Cells*, D. H. Doughty, B. Vyas, T. Takamura, and J. R. Huff, Editors, PV 393, p. 151, Materials Research Society, Pittsburgh, PA (1995).
4. G. C. Wei and J. M. Robbins, *J. Am. Ceram. Soc.*, **64** (5), 691 (1985).
5. T. M. Besmann, B. W. Sheldon, R. A. Lowden, and D. P. Stinton, *Science*, **253**, 1104 (1991).
6. P. Delhaes, *Chemical Vapor Deposition. Proc. Fourteenth Intl. Conf. and EUROCV D 11*, M. D. Allendorf and C. Bernard, Editors, PV 97-25, p. 486, The Electrochemical Society Proceedings Series, Pennington, NJ (1997), -495.
7. S. Bammidipati, G. D. Stewart, J. R. Elliott, Jr., S. A. Gokoglu, and M. J. Purdy, *AIChE Journal*, **42** (11), 3,123 (1996).
8. J. E. Ritter, K. Jakus, A. Batakis, and N. Bandyopadhyay, *J. Noncrystalline Solids*, **38-39**, 419 (1980).
9. F. F. Vitman, and V. P. Pukh, *Aavodskaya Laboratoriya*, **29**, 863 (1963).

Table 1. Material property targets and values.

Property	DOE Target	POCO Graphite	Carbon Composite
Bulk conductivity (S/cm)	>100		200-300
Surface resistivity (W/cm)	N/A*	8	12
Hydrogen permeability (cm³/cm²-sec)	<2 x 10 ⁻⁶	Meets target	Meets target
Corrosion rate (mA/cm²)	<16	80	6
High volume production cost (\$/kW)	<10	40	5.50

*Not available

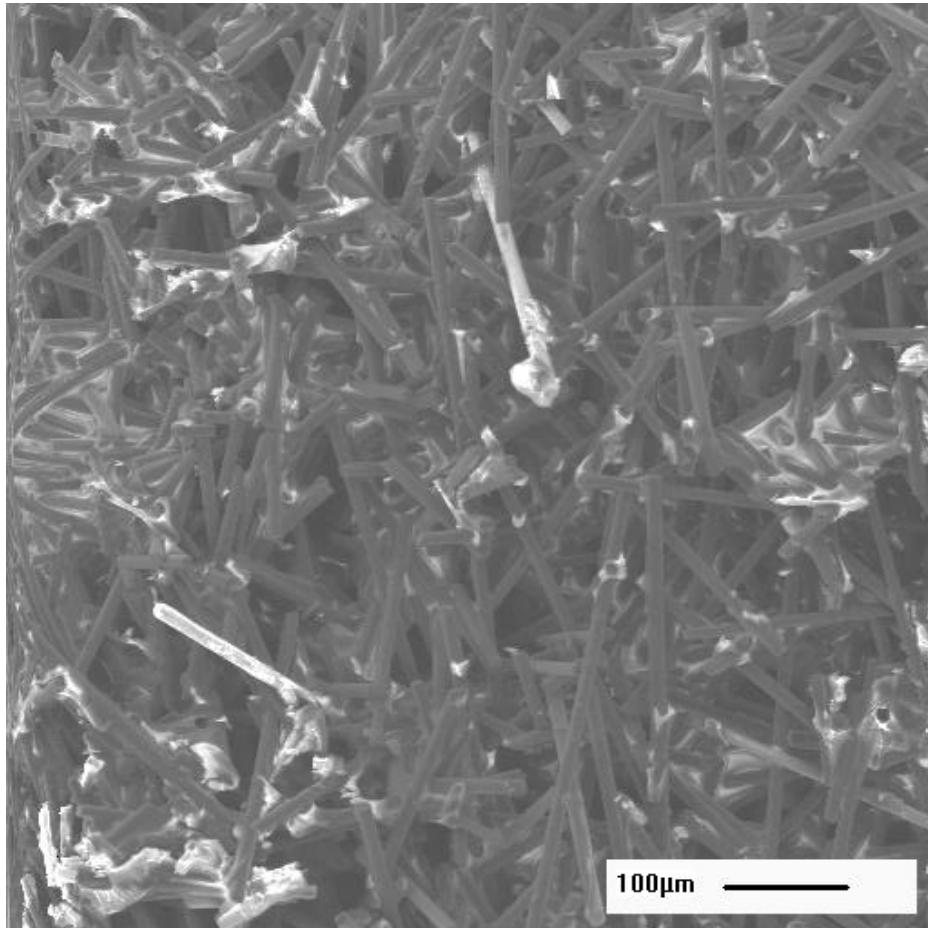


Fig 1. SEM image of the slurry-molded carbon fiber preform prior to infiltration.

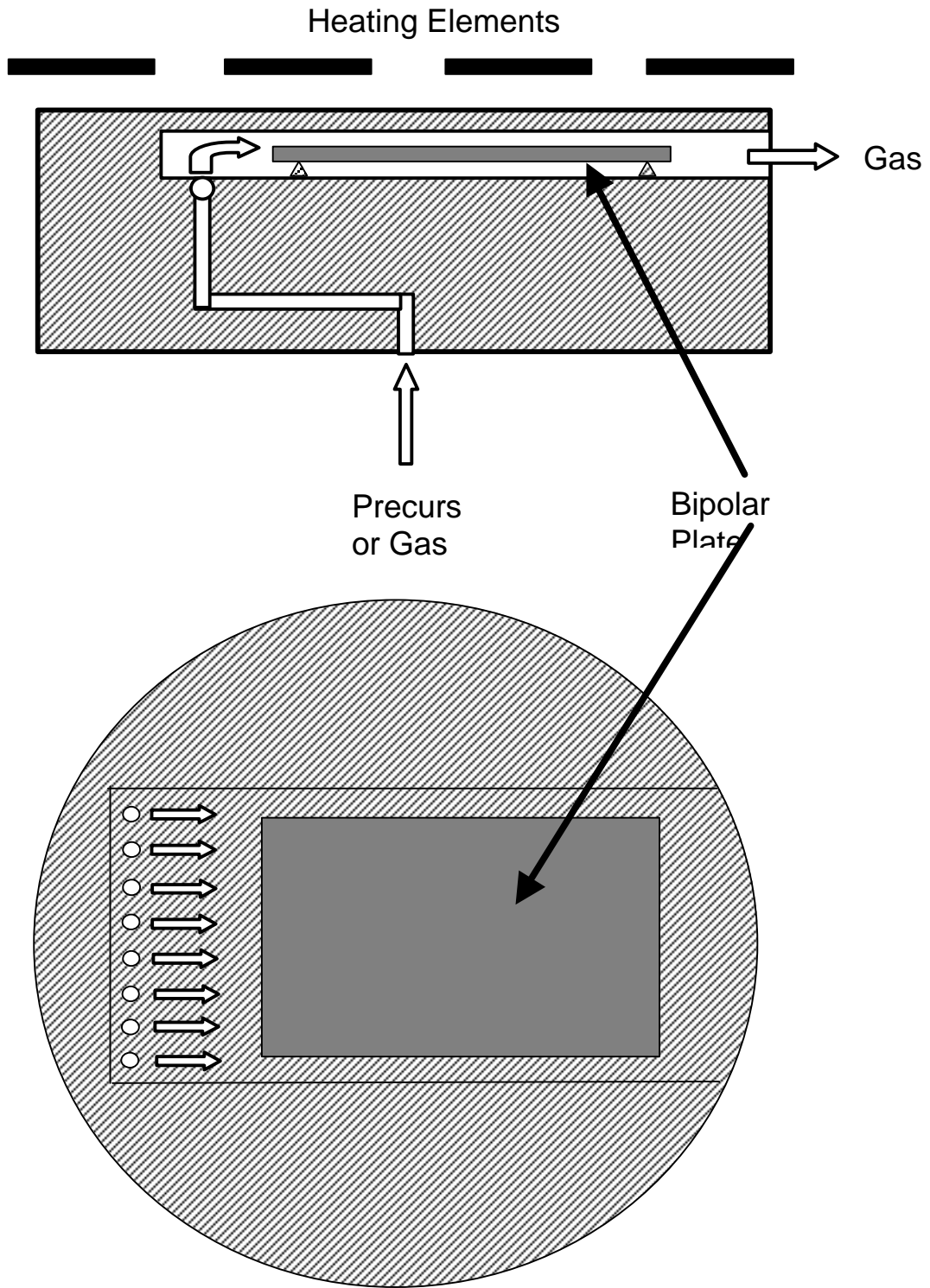


Figure 2. Top and side views of the fixture used for infiltrating the preforms showing the gas flow path.

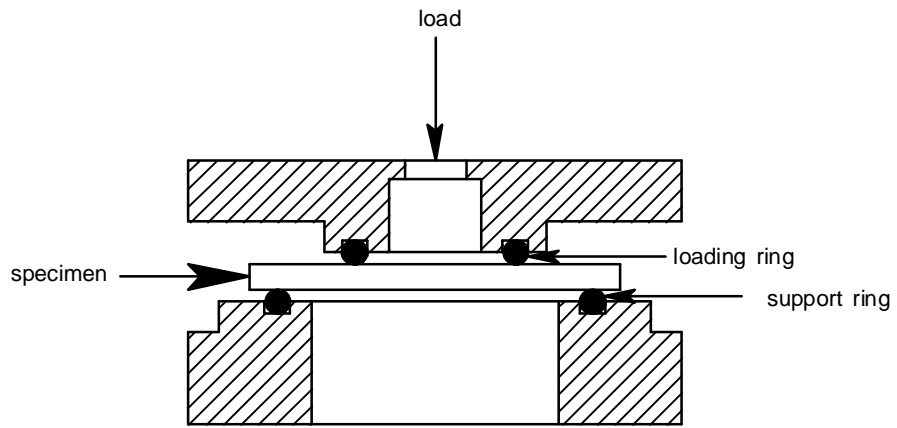


Fig. 3 Biaxial test fixture.

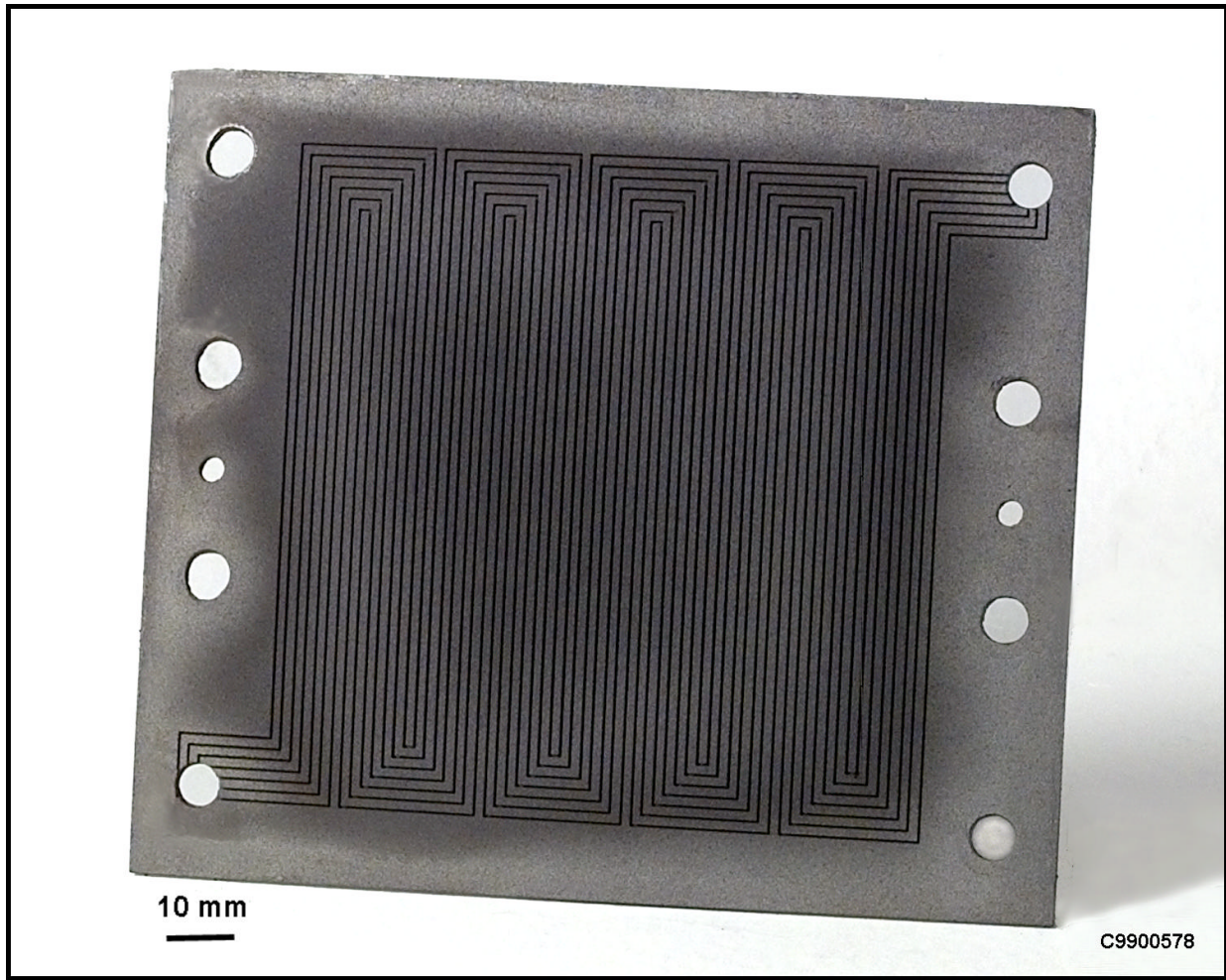


Figure 4. Prototypical Los Alamos National Laboratory-design, 100-cm² active area carbon/carbon composite bipolar plate showing the flow fields and other features

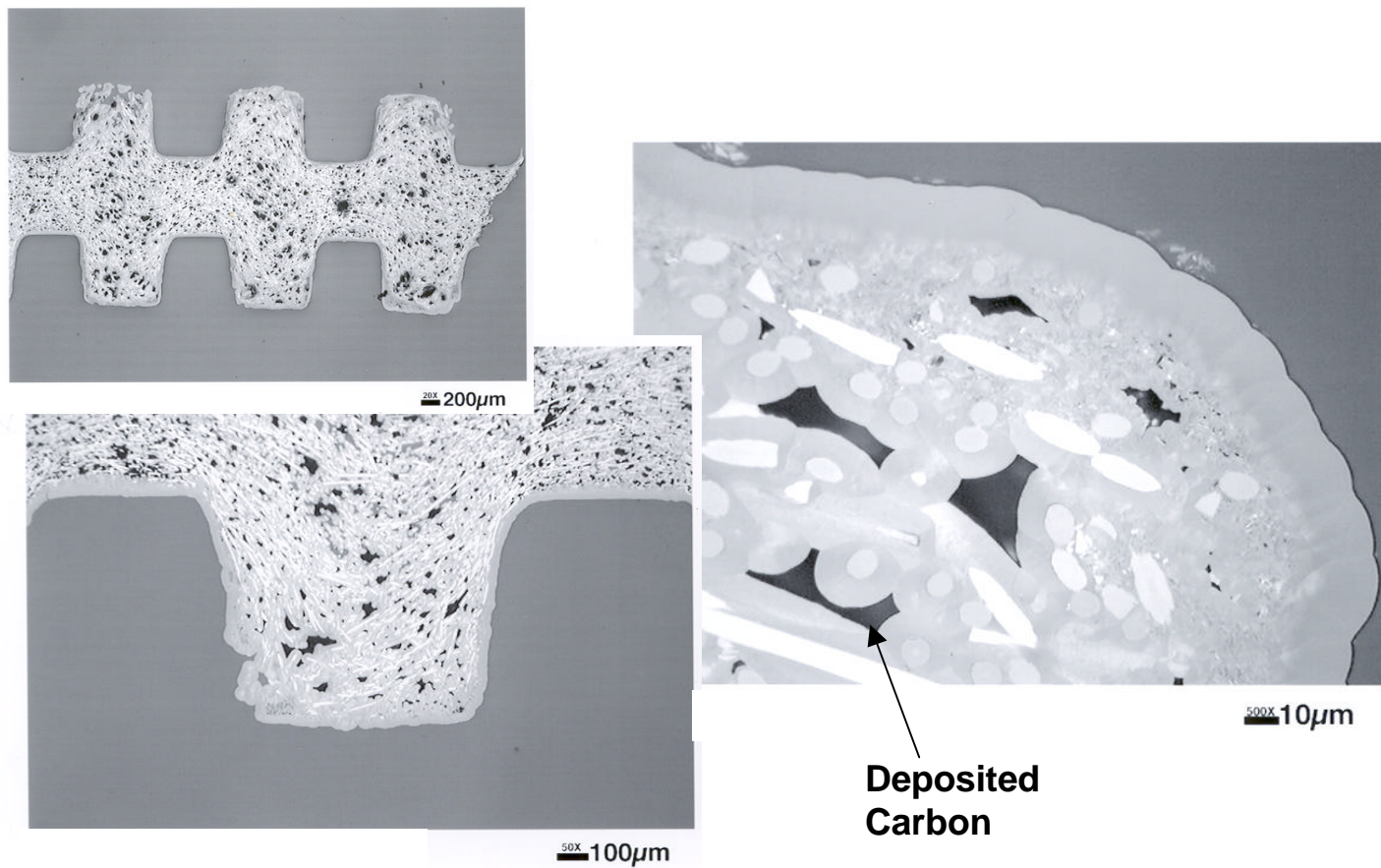


Figure 5. Prototypical Los Alamos National Laboratory-design, 100-cm² active area carbon/carbon composite bipolar plate showing the flow fields and other features

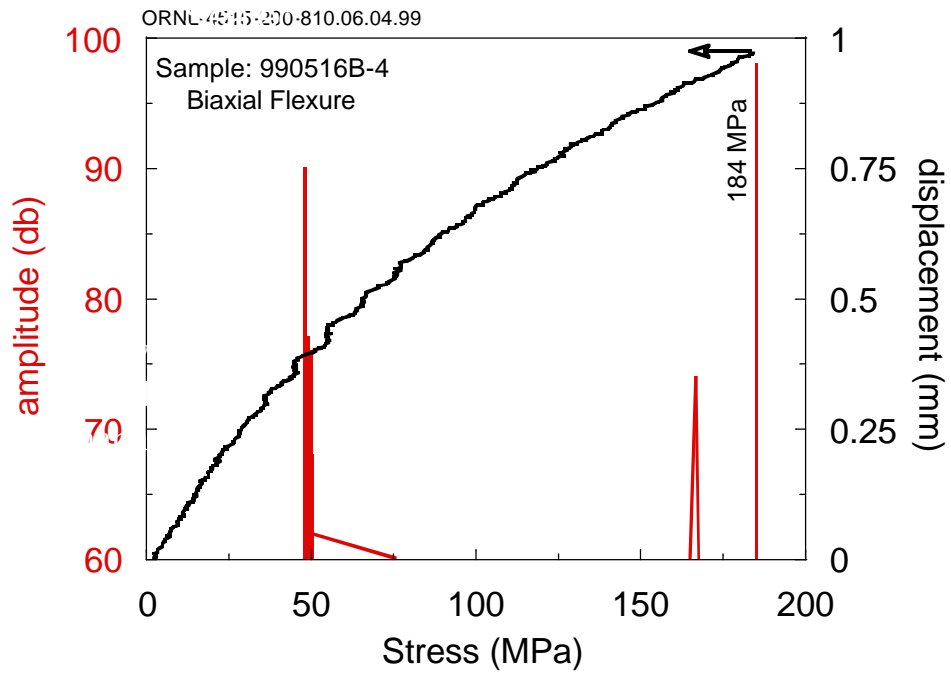


Figure 6. Stress versus cross-head displacement curve for the biaxial flexure testing of a carbon/carbon composite sample also showing the acoustic emissions detected during loading that are caused by crack formation in the sample.

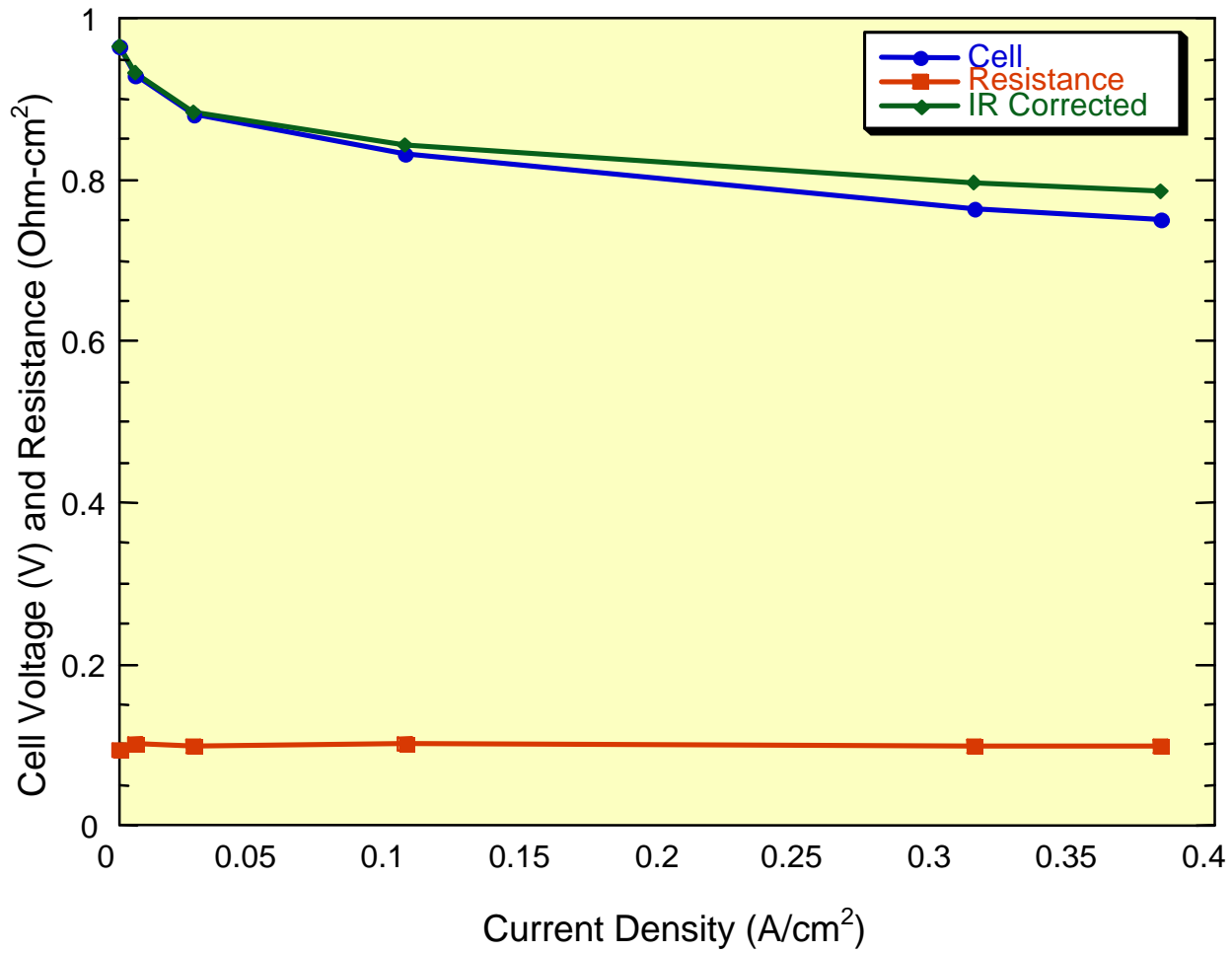


Fig. 7. Cell resistance and current-voltage measurements for the 100-cm² active area carbon composite bipolar plate.